

Received December 3, 2020, accepted December 28, 2020, date of publication January 4, 2021, date of current version January 22, 2021.

Digital Object Identifier 10.1109/ACCESS.2020.3049116

Downhole Telemetry Systems to Monitor Electric Submersible Pumps Parameters in Oil Well

**DIEGO ANTONIO DE MOURA FONSÊCA¹, ANDRÉS ORTIZ SALAZAR¹, (Member, IEEE),
ELMER ROLANDO LLANOS VILLARREAL², (Member, IEEE),
GERMAN ALBERTO ECHAIZ ESPINOZA,³ AND
ALAN CÁSSIO QUEIROZ BEZERRA LEITE⁴**

¹Department of Computer Engineering and Automation, Federal University of Rio Grande do Norte (DCA-UFRN), Natal 59072-970, Brazil.

²Department of Natural Sciences, Mathematics and Statistics, Federal Rural University of the Semi-Arid (DCME-UFERSA), Mossoró 59625900, Brazil

³Department of Electronics Engineering, Universidad Nacional de San Agustín de Arequipa, Arequipa 04001, Peru

⁴Renewable Energy Department, Federal University of Ceará (CCTSSER-IFCE), Juazeiro do Norte 63040-540, Brazil

Corresponding author: Elmer Rolando Llanos Villarreal (elmerllanos@ufersa.edu.br)

This work was supported in part by the Comissão de Aperfeiçoamento de Pessoal do Nível Superior (CAPES), in part by the Conselho Nacional de Desenvolvimento Científico e Tecnológico (CNPq), and in part by the Universidad Nacional de San Agustín de Arequipa (UNSA) Investiga under Grant IAI-019-2018-UNSA.

ABSTRACT The electrical submersible pump (ESP) is widely used in the oil industry as an artificial lift method in deep wells, and its primary application of ESP is to increase the oil flow rate. Information such as the pump intake and discharge pressure, the oil reservoir and motor winding temperature, etc., provide critical data necessary to ensure proper ESP system operation and optimize production. In this article, an ESP downhole parameter monitoring system is proposed. Potentiometers are used to generate analog signals, emulating the analog sensors. The information is sent up to the surface based on the current loop through the same power cable by DC signals overlapping to AC signals in the proposed design. The article details the construction of the communication protocol and electronic circuits used in telemetry. The tests were carried out in an oil-producing company to validate the proposed telemetry system's reliability and accuracy. The good results of the robust design demonstrated it to be a promising downhole sensor for industrial applications.

INDEX TERMS Electrical submersible pump, downhole monitoring tool, submersible motor, power line communications, current loop.

I. INTRODUCTION


Information such as downhole pressure and temperature are valuable in order to optimize production and also help in identifying or avoiding problems that may lead to an undesired shut-down of an oil well [1].

As important artificial lifting equipment, electric submersible pumps perform an irreplaceable role in the secondary and tertiary oil recovery, which puts forward higher requirements for the application reliability of electric submersible pumps [2]. The electric submersible pump (ESP) has been widely used in oil fields [3] for its advantages of high lift, large displacement, and convenience for management [4].

The total number of oil wells worldwide utilizing some method of artificial lifting is around 95%, the most common

being the Mechanical Pump (BM), with 74% of the total number of these facilities, followed by the ESP [5]–[7], with an amount ranging from 150 to 200 thousand wells in operation [8]. Despite the second position in terms of facilities, ESP is the system with the highest sales, 54% of the artificial elevation market representing in 2014 43% of the global annual expenditure in that market. [5]. Considered the best choice when high production volumes are required, ESP is typically used in wells with a production of 200 to 20,000 barrels of oil per day, although it is a high-cost method. [5], [9]–[11].

In low price season, it is indisputable that producing wells operate efficiently to provide at a lower cost per barrel. Information such as downhole pressure and temperature are valuable in order to optimize production and also help in identifying or avoiding problems that may lead to an undesired shut-down of an oil well. Observation of the operating

The associate editor coordinating the review of this manuscript and approving it for publication was Mauro Fadda .

conditions of downhole equipment, such as the motor and pump, is carried out by installing a set of sensors close to the downhole. Thus, parameters such as pump intake and discharge pressure, motor temperature, produced oil temperature, vibration, contamination of the engine insulating oil, and current leakage are collected by the set of sensors at the bottom of the well and transmitted to the surface through a communication system to be processed. Through the use of these ESP operating parameters, it is also possible to understand the behavior well and ESP as a system. Such understanding leads to better system design and a continuous improvement process based on measured data known. Onshore ESP wells can achieve a depths from 500 to 4,000 meters [10], [12]. It is impracticable to lay an extra cable for powering the measurement system due to costs with extra materials and human resources. Besides, exist the chance of increasing the failure of the component [12], [13]. The most natural alternative in this situation is to use the three-phase cable itself that feeds the ESP motor as the physical medium to transmit the data to the surface [12], [13].

The data obtained from the downhole sensor will allow obtaining a direct measurement of ESP and evaluate the ESP system's performance trends, including the production field. These trends alert experts to the occurrence of possible problems with surface and subsurface equipment in advance, in time to take corrective measures [14], preventing the premature system failure. A forced shut down due to a failure that requires the replacement of one of the constituent components of the ESP system can cost from US\$ 15,000 to US\$ 40,000 [15]. Also, the production stoppage results in a loss of revenue, which is often more expensive than the amount spent on the equipment and services associated with its replacement [16]. Also, Operators can use a downhole sensor to determine operating parameters in completions with ESP pumps and increase pump lifting efficiency while controlling the pump operating time. Therefore, it is of great significance to carry out the research on the theory and technology for fault diagnosis of the ESP [4].

The most used downhole monitoring tool design in the field downhole utilizes a DC communication signal transmitted over the three phases of the downhole main power cable. The structure conceived in served as a basis for the development of several telemetry systems that either used the structure initially proposed or suggested a new topology with small basic structure changes [17], [18]. Another communication strategy is through modulating high-frequency signals to transmit information from the motor/pump system at the bottom of the well. This method has higher transmission rates and tolerance to SLG (single-line-to-ground) faults compared to the dc communication scheme [13]. Despite the high transfer rates and mitigating the SLG problem, this technique has a current limitation of the system's constructive character. The impedance imposed by the physical environment and the harmonic filter (installed in VSDs in ESP systems) will cause a strong attenuation in the high-frequency signals. As a consequence, the signals will

be uncharacterized, and, therefore, their transfer will be compromised.

Aiming to overcome major drawbacks and limitations of the two existing downhole monitoring tool design methods in 2015 [13] proposed a phase-to-phase communication scheme using power-line communication technique known as a "two-way automatic communication system (TWACS)" for the downhole monitoring tool design. On that occasion, two case studies are conducted using a real ESP system under normal and single-line-to-ground fault conditions. Following the same idea, in 2017 [12], suggested a downhole tool design method using a phase-to-neutral communication scheme in which an effective signal communication path is formed by external impedance on the wellhead connecting one phase to the ground combined with a controlled thyristor at downhole connecting the neutral of an electrical submersible motor to the ground. The performance of the method is evaluated using simulation through the case and sensitivity studies.

In this article, it is implemented a downhole telemetry system's complete solution uses a DC signal (digital pulses) over three phases of the main power cable to transmit data between the downhole module and the surface monitoring electronics unit. It is proposed a new communication protocol, based on the Manchester coding, which guarantees the data from the parameters measured at the bottom of the well reach the surface module to be read. The protocol transfer rate was established based on impedance analysis of the three-phase cable that powers the motor. Details of the construction of the protocol, as well as the telemetry system, are presented. The validation of the proposed protocol, implemented in the telemetry system's transmission and reception modules, was performed through tests in an oil well using the ESP elevation method. At the time, the performance of the proposed solution was evaluated for different values of motor frequency.

II. MATERIALS AND METHODS

A. ESP EXPERIMENTAL SETUP

The experimental setup reproduces the electric drives and controllers project system of the ESP artificial lifting method. The main components in the proposed setup include a variable speed drive (VSD) and a three-phase wye-connected choke, both as surface electronic devices. Besides, a three-phase power cable feeding main AC power to the motor and an ESP motor makes up the subsurface units. The Figure 1 shows a snapshot of the experimental setup.

The field tests were planned in a pilot well with ESP installation. The well where the tests will be carried out has a depth of 30 meters with a diameter of the 13.5/8". However, from the well, the subsurface modules (cable and motor) were not used. In other words, a 2036 m motor power cable and an ESP motor, both on the surface, were used. In this way, it was possible to connect our bottom sensor to that motor on the surface. Regarding our surface module, it was connected directly to the well surface filter. Its surface unit has a set of four protection and monitoring modules, in addition to the Human Machine Interface (HMI). On the subsurface, is the

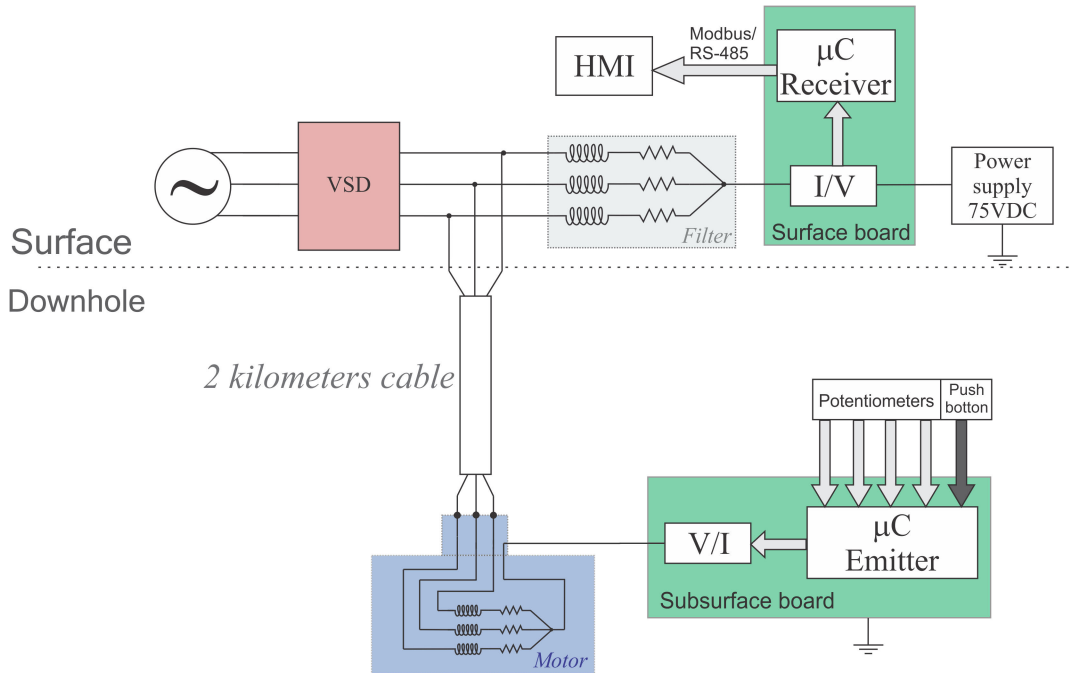


FIGURE 1. The structure of the communication system.

the motor. The Table 1 presents the characteristics of the equipment used in the tests. This basic well structure makes it possible to evaluate the ESP system for several different conditions, that is, the use of different inverters, as well as cables of different sizes, diameters, and shapes (flat or round).

TABLE 1. Units for Magnetic Properties

Equipment	Parameter
Transformer	Dry Type, Power Rating 125 kVA, Primary Voltage 420-480 V, Secondary Voltage 900-1400 V
Power cable	AWG#2, 5 kV, round construction, 2,236 m
ESP Motor	80 HP, 440 V, 101 A a 60 Hz
Variable speed drive	150 kVA, active filter, nominal current 242 A, switching frequency 2 kHz
Variable speed drive (no active filter)	110 kVA, 440 V, nominal current 124 A, switching frequency 4 kHz

The power cable connects the variable frequency drive to the AC motor to transmits the required surface power to it. In [19] was presented the modeling of the 2036 m ESP power cable used in field tests. The electrical parameters of the cable, such as impedance, phase, inductance, and capacitance, were obtained through the Keysight impedance analyzer E4990A. Five hundred points were collected with the following information: frequency, absolute value, and phase, which served to characterize and model the cable.

A VSD can control the submersible electrical motor at a speed that the well produces with the greatest efficiency and keeps the ESP within its best efficiency range [8]. The VSDs also offer soft motor starting for ESP systems and reduce

the impact to power grid during the motor start-up [20]. The drive allows the pump to be operated continuously or intermittently or be shut off in the event of a significant operational problem. The direct speed control afforded by the VSD increases system efficiency and the run life of the ESP system while reducing the incidence of downtime [8]. The main advantage of the VSD is that it allows the operator to change the speed of the ESP to account for uncertainty in the productivity index of the well or changing well conditions. The VSD works as a power supply, generating frequency and resonance values according to the curve that relates frequency and output voltage.

The surface induction power is a set of three-phase inductors in star connection ungrounded system. Also known as choke panel, it is the interface between the ESP power system and the surface electronics equipment, filtering the digital communication signal from the AC power line [21]. The purpose of the surface choke is to allow the ESP Gauge Interface to provide power to and communicate with the downhole tool, in the later case creating a virtual ground via WYE point for direct connection for downhole communication.

The schematic diagram of the surface filter is shown in Figures 2, 3:

The artificial star point is constructed by a three-phase electric reactor with the same three-phase winding parameters as the downhole motor, which supplies power for the downhole monitoring circuit based on the principle of star point equipotential [2]. The electronic surface unit connects to the downhole tool via the motor power cable through the choke. This electronic module is connected to the choke wye point and the wellhead ground. Likewise, the downhole

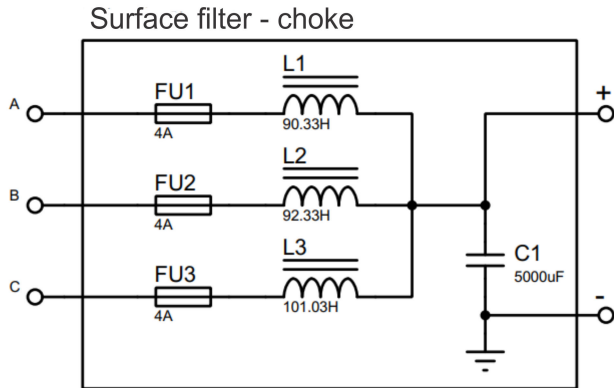


FIGURE 2. The three-phase inductors at the surface: Choke diagram.



FIGURE 3. The three-phase inductors at the surface: Real choke.

electronic module connects to the neutral of the ESP motor and the downhole system’s ground through the well casing. The neutrals of the choke and the ESP motor are ungrounded. Meanwhile, a loop for current signal transmission was established, eliminating the need for an extra communication cable [22], [23]. The downhole sensor sends the data as a train of current pulses to the surface. In this way, the downhole unit is equivalent to a current source under the control of the uphole group in series with a resistance [11]. The current loop shows strong anti-interference and high reliability because the influence of line impedance, cable length, voltage drop as well as noise interference is negligible when transmitting data in this way. Therefore, the current loop is suitable for long-distance data transmission [24].

The Figures 3–6 provide a panoramic view of the test system together with the proposed electronic modules.

B. PROPOSED TELEMETRY SYSTEM

The telemetry system consists of five electronic modules. These modules collect information from the sensors installed in the subsurface equipment, located at the bottom of the well, processing them and sending them to the surface. On the surface, the data will be made available for monitoring and analysis. The block diagram illustrated in Figure 7 shows the layout of these modules and how they are interconnected.

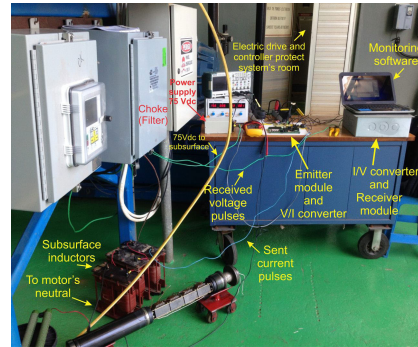


FIGURE 4. The experimental setup overview.



FIGURE 5. ESP components: Motor-pump assembly installed horizontally.



FIGURE 6. ESP components: Three-phase power cable.

1) AUXILIARY POWER SUPPLY

The three-phase wye-connected choke on the wellhead and the motor are linked in parallel, as shown in Figure 8. This feature ensures that both neutrals point (choke and motor) are kept at the same relative potential.

The artificial star point is constructed by a three-phase electric reactor with the same three-phase winding parameters as the downhole motor, which supplies power for the downhole monitoring circuit based on the principle of star

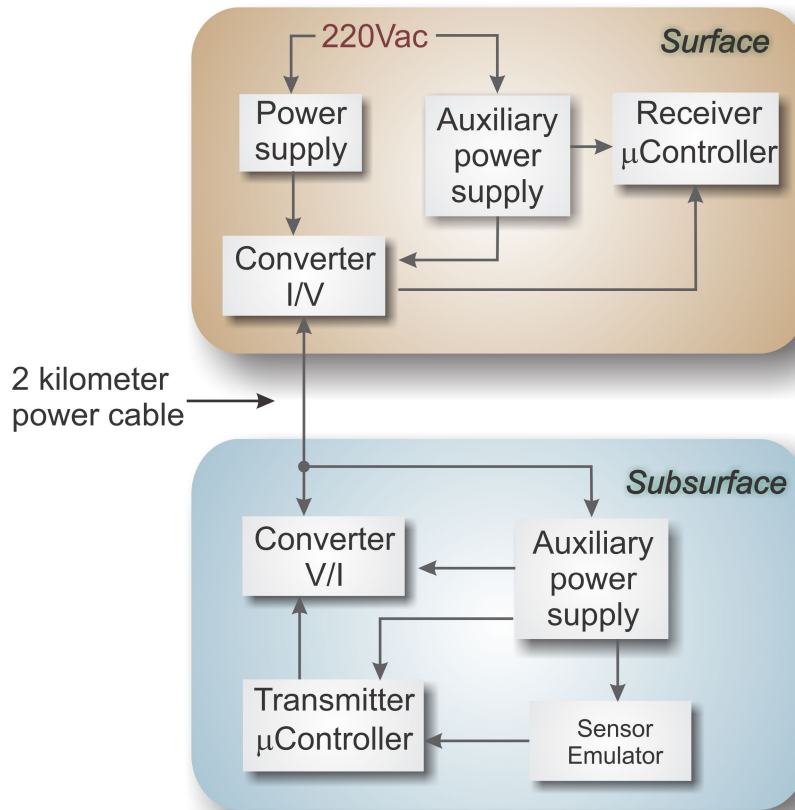


FIGURE 7. The block diagram of the proposed system.

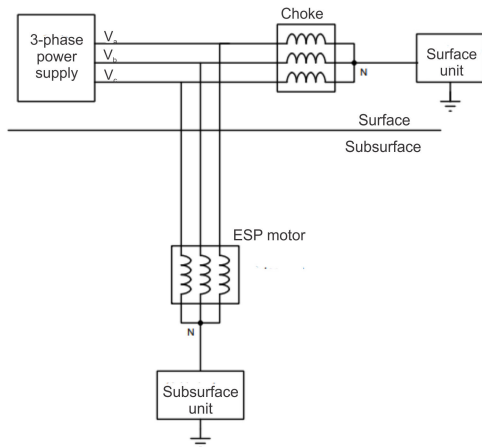


FIGURE 8. Schematic diagram of energization of subsurface electronics.

point equipotential. At the surface, the electronics module includes a $75 V_{dc}$ power supply that provides DC voltage to the downhole electronics module. The surface electronics unit is connected to the neutral of the choke. This way, the $75 V_{dc}$ reaches the upper end of the power cable and, consequently, the motor’s neutral. The motor’s neutral wire is connected to the voltage regulator circuit that supplies DC voltage levels of $5 V_{dc}$ and $15 V_{dc}$ to the electronic subsurface

modules. Such operation characterizes the circuit as a subsurface source, terminology that will be used throughout the article. The Figure 9 depicts the power source circuit diagram.

For protection measures and to prevent that alternating motor current may cause communication interference between downhole and uphole unit, the source circuit is connected to the motor neutral via a large inductor, which can reach the value of 120 H [23]. Therefore, the alternating current flowing from the surface through the ESP power cable and the motor is filtered by this inductor so that the data signals can be transmitted without any alternating current influence. In the testbed used for the experiments, three inductors in series with an equivalent inductance of $L_{eq} = 53.4 H$ represent the mentioned inductance.

2) TRANSMITTER DEVICE

The data acquisition and transmission circuit collects data from the sensors installed in the subsurface equipment, analyze, process, and send the acquired data to the receiver module, on the surface. For practical purposes, the analog and digital signals related to downhole sensors will be generated by potentiometers and an on-off switch in this research. The Figure 7, at the bottom of the well, shows a block diagram illustrating how the transmitting circuit is associated with the other components. The Microchip PIC 18F4550

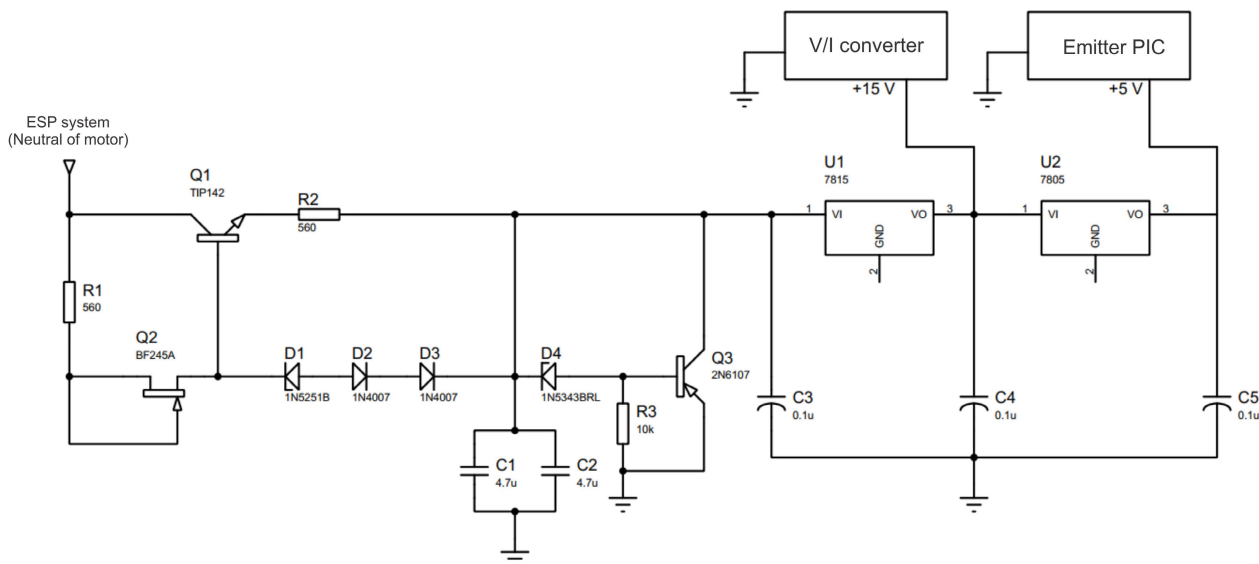


FIGURE 9. Circuit diagram of the auxiliary power supply.

microcontroller was chosen because it has technical requirements that meet the application. Among the elements is compatibility with the SPI communication protocol, the quantity of analog and digital inputs, in addition to the low cost.

An ESP well running with a downhole monitoring tool, the downhole parameters usually monitored include: pump intake pressure and temperature, motor oil or motor winding temperature, pump discharge pressure. Some modern downhole monitoring tools have inputs for vibration and electric current leakage signals, which allows cable degradation to be determined.

Another critical parameter is the contamination of insulating oil in the motor applied to the electrical submersible pump which indirectly protects the induction motor associated with that system [25]. The seal with the continuous work causes the onset of motor oil contamination, which leads to the loss of its insulating property. The statistics show that the induction motor has the highest failure rate by oil contamination. This contamination causes problems to the induction motor due to short-circuiting.

The data acquisition process begins when the information from the potentiometers arrives at the microcontroller ADC pins. The pic microcontroller 18F4550 has an inbuilt 10-bit resolution ADC. The temperature and pressure data are stored in the internal microcontroller RAM. However, due to data volume generated by the vibration sensor (x and y axes) was necessary an external RAM. On the contrary, the contamination sensor signal is sent to a digital input indicating whether or not the insulating oil is contaminated.

a: COMMUNICATION PROTOCOL

The physical topology of the proposed telemetry system is point-to-point. The three-phase motor power cable and the downhole sensor ground (or well casing) constitute the

current loop, i.e., the physical medium. The transmission is unidirectional (or simplex) so that only the sender device sends the data.

Due to the impossibility of using an external clock, we opted for the use of a self-synchronized signal, which includes synchronism information in the transmitted data. Guaranteed transitions each bit period, even in the event of long sequences of 1s or 0s, enables straightforward recovery of the clock and data signal by the receiver. Another relevant factor in digital communication is the DC components, that is, if the data has a long sequence of zeros and the average signal strength becomes distorted. Thereby, the receiver may have trouble distinguishing between a bit zero and bit one.

The polar line coding (NRZ, RZ, Bi-phase Manchester, and differential Manchester) have characteristics that meet the needs imposed by the scenario found in the ESP system. In this case, it was decided to use the bi-phase Manchester encoding to implement the protocol. There is always at least one transition per bit period to enable clock recovery by the receiver. Figure 10 illustrates the behavior of a bit sequence sent by the Manchester method. In this application, low-to-high transitions are received as binary ones, high-to-low transitions as zeros. Figure 10 shows that each bit has a positive and negative contribution in terms of voltage, eliminating the DC components. However, The Figure 10 also demonstrates a disadvantage of Manchester encoding: it is necessary a transition for every bit, which means two Manchester logic states are used to convey one standard logic state. Thus, twice as much bandwidth is needed to transfer data at the same rate. However, compared to the benefits obtained with the encoding Manchester, this limitation does not compromise the protocol’s performance.

The protocol provides two different frame types. The first, called “regular sensors”, encapsulates information from

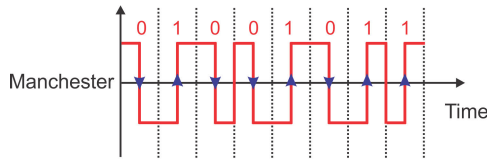


FIGURE 10. Manchester encoding.

four analog variables (for example, two temperatures and two pressures) and one digital variable (insulating oil contamination). The second frame, denominated “special sensors”, encapsulates the data generated by the accelerometers. The frame size is variable, depends on the number of installed instruments. The minimum frame size is 42 bits, sending data from a single sensor, and 117 bits considering the five sensors. Figure 11 shows how the fields are organized in the table that encapsulates the data.

Start Bit 1 bit	varCount 3 bits	Data 19 - 95 bits	CRC 16 bits	Stop Bit 2 bit
--------------------	--------------------	----------------------	----------------	-------------------

FIGURE 11. Frame format for pressure, temperature and contamination variables.

In addition to the fields referring to the values of the variables, the structure has the following control fields:

startBit: 1 bit signals the start of the frame

varCount: 3 bits indicating the number of variables to be sent.

data: the size varies from 19 to 95 bits, according to the number of sensors read.

CRC: 16 bits that indicate the value of the CRC (cyclic redundancy check) used to detect transmission errors.

stopBit: 2 bits signal the end of frame transmission.

Figures 12 and 13 exemplify the data frame format to send one and two variables, respectively. The first one is an illustration of the data field for one sensor. The first 3 bits to identify the sensor and 16 bits to store the value read from it. The Figure 13 depicts the case of reading two sensors. In this respect, the first 19 bits refer to the first sensor, and the following 19 bits relating to the second one. Both data field are with the identification field, followed by the read value field.

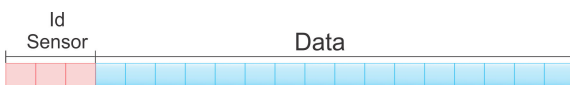


FIGURE 12. Frame structure for sending regular sensor information. Organization of the data field for sending values from: one regular sensor.

The second frame, denominated “special sensors”, encapsulates the data generated by the accelerometers. The frame has a fixed size of 69 bits. It was modified to suit the content of the information to be sent. The vibration message is transmitted simultaneously on both the X and Y-axis. The control field is 22 bits wide, as in the regular sensor’s frame.

The difference from that is the number of bits in the data: 19 up to 95 for regular sensors against 47 for the special one. The format of a vibration data frame is shown in Figure 14 where,

startBit: 1 bit that signals the start of the frame

varCount: 3 bits indicating the number of variables to be sent.

data: it is divided into smaller fields and has a size fixed at 47 bits, of which 3 bits define the sensor, 12 bits identify the packet, and the remaining 32 bits store the read values, 16 for each coordinate.

CRC: 16 bits that indicate the value of the CRC (cyclic redundancy check) used to detect transmission errors.

stopBit: 2 bits signal the end of frame transmission.

The data field in the described frame has that structure because it is needed to store 4 thousand vibration points acquired data in 1 second for each coordinate. The microcontroller is limited in memory to send this volume at once. In this case, the acquired data is fragmented to fit into the data field, and in each packet sent, a piece of vibration information is transported. For the purpose of providing sequence control, each packet is given a 12 bits sequence number. Since this field is just 12 bits long, it identifies 4096 frames. The 12 bits id field provides a mechanism for the receiver to reassemble the complete vibration message. Figure 15 shows the described field.

b: DOWNHOLE SENSOR INFORMATION - ESP

Each downhole equipment will have a unique serial number. From that information, it will be possible to track it through data such as location, operating time, and category to which it belongs. The class indicates which and quantity of sensors in the equipment. The possible sensors are temperature, pressure, contamination, and vibration. Therefore, when in operation, the sender’s first action is to transmit this information to the receiver and then start the sensor data acquisition process. As there is no bidirectional communication between the communication modules, which would allow a request in case of an error in the received package, this information is sent twice in a row at the beginning and specific periods.

c: ACQUISITION AND PROCESSING OF ANALOG AND DIGITAL PARAMETERS

The data acquisition process begins after sending the identification information to the surface microcontroller. Electrical signals from the temperature and pressure sensors are fed into a 10-bit built-in ADC converter, which digitizes these analog signals into their computer-compatible equivalent. There is no signal conditioning circuit because the potentiometers used to emulate the sensors generate signals from 0 to 5 V. The downhole module will be located in an environment subject to noise, mechanical vibration, and high temperatures. Thus, for each sensor, a certain number of acquisitions is performed, and the arithmetic mean is calculated. The number of readings is defined by the number of unused bits after the A/D conversion. In other words, the 10 bits resulting from the



FIGURE 13. Frame structure for sending regular sensor information. Organization of the data field for sending values from: two regular sensors.

Start Bit 1 bit	varCount 3 bits	Data 47 bits	CRC 16 bits	Stop Bit 2 bit
--------------------	--------------------	-----------------	----------------	-------------------

FIGURE 14. Frame structure for vibration data.

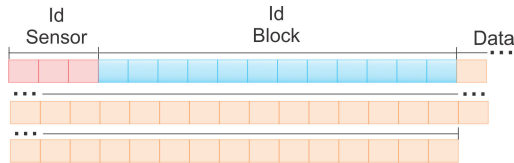


FIGURE 15. Organization of the data field for sending vibration values.

A/D conversion are stored in a 16-bit variable, thus leaving 6 “free” bits, which allows the sum of 64 readings of that sensor. In the end, this sum is divided by 64 to obtain an average of 10 bits.

A 10-point moving average filter is responsible for smoothing the acquired values, and therefore to reduce the noise effect. The moving average filter is a simple Low Pass FIR (Finite Impulse Response) filter commonly used for regulating an array of sampled data/signals. It is optimal for reducing random noise while retaining a sharp step response. In this application moving average filter takes ten samples of the previously calculated values in the arithmetic average at a time and takes the average of those to produce a single output point. Each provided point is stored in the array called “data vector”. Once filled, the content of the data vector is copied to the data field of the data frame, and together with the control fields, will form the vector that will carry the data to the surface. The Figure 16 represents the acquisition and processing steps.

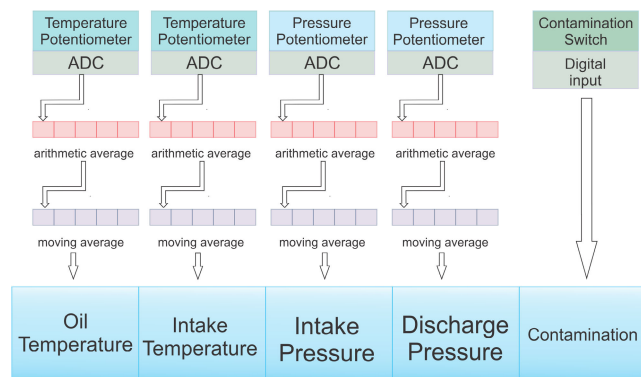


FIGURE 16. Data frame assembly steps.

The acquire information regarding the vibration frequencies process follows the same steps as the analog

data acquisition process. The differences in the forms of acquisition are the volume and speed at which the vibration data is read. Two potentiometers emulate the accelerometers, one for the x-axis and one for the y-axis. From each of these 4,000 points will be obtained in 1 second. Although each potentiometer is connected to a channel, the microcontroller has a single A/D converter. Therefore, the reading of each analog input is done through a switch, whose frequency is fast enough so that there is no loss of information read. The conversion process ends only when it reaches 8 thousand points. The MCU does not have enough RAM to store a large amount of vibration data at the same time. The solution was incorporating an external memory chip. The Microchip 23K256, with 256 Kbits (32 KBytes) of memory, provides storage for the application. The module is connected to the microcontroller board through the serial interface. The option for serial communication was due to the pin limitation of the microcontroller. However, the serial writing time in memory could be seen as a complicator in the process of acquiring the vibration data. This possible limitation was overcome with using a 32 MHz quartz crystal, thus providing resources for the configuration of the A/D converter and the writing process of 8 thousand points within 1 second.

The points of the X and Y coordinates are stored in RAM as follows: the four thousand points referring to the X coordinate occupy the first eight thousand positions (0000h to 1F3Fh) and the other four thousand referring to the Y-axis, the following eight thousand locations (1F40h to 3E7Fh). The writing in memory occurs sequentially and not in batch, so, after reading a point X, a point Y is read, and then writing occurs. This process repeats up to acquiring the 8 thousand points.

After the data storage generated by the accelerometers is completed, the data treatment step to send them to the receiver begins. The protocol frame is a series of bits composed of information from a single pair of XY coordinates. Therefore, it is necessary to assemble 4,000 frames to send a 1-second acquiring of the vibration variable. The 12-bit identifier (4096 identifiers) allows the correct reassembly of the segments to ensure that the packages are assembled to form the original information.

The sending of the vibration frames alternates with the frames of conventional sensors. Once the sending of the vibration data is complete, a new cycle of data acquisition and treatment begins, repeating the entire process.

The data transfer rate of such systems is limited by the electrical impedance of the motor windings and the power cable.

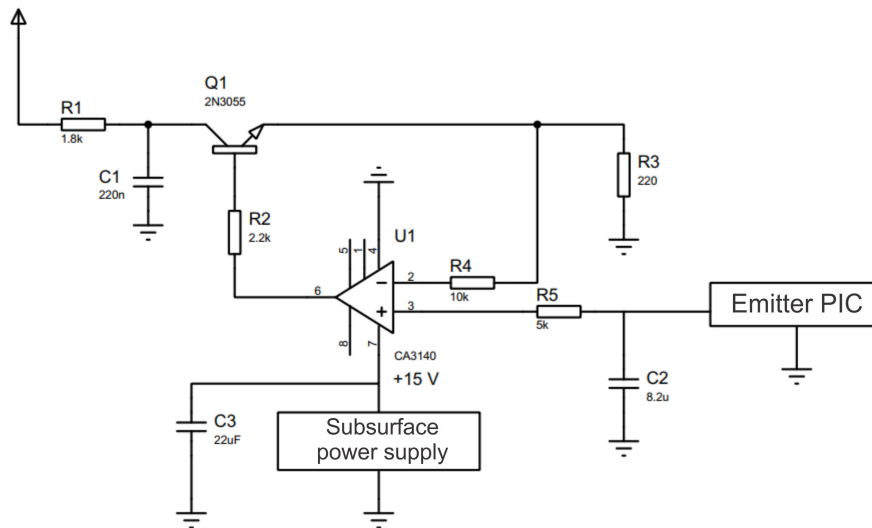


FIGURE 17. Circuit diagram of voltage to current converter.

3) SUBSURFACE COUPLING

As described in section about choke, the system ground will serve as the signal return path to the surface. The data packages are sent to the surface as a current signal, whereas the cable length for the ESP wells can reach 4000 m [10], [12]. Under these conditions, the voltage signals would have attenuated due to the cable length. Alternatively, the current signal does not present any loss considering the same scenario, in addition to having low sensitivity to electrical noise and not having its accuracy affected by the voltage drop in interconnections. However, the power cable length and the electrical impedance of the motor windings limit data transfer rate of the such system. A more precise analysis of the physical layer, in which only the three-phase cable was considered. The cable length was 2036 meters, three-phase 4 AWG, and a flat profile. The analysis showed that the cable acts as a low-pass filter with a cutoff frequency of 10Hz [19].

4) VOLTAGE TO CURRENT CONVERTER (V/I)

The emitting module’s micro-controller generates a square voltage signal whose amplitude is $5V_{dc}$, and the baud rate is 10 bps. The voltage-to-current converter shown in Figure 17 converts the voltage signal generated by the PIC into a square current signal with approximately 500mA amplitude and the same frequency as the voltage signal.

The circuit works as follows: the emitting microcontroller, connected to the non-inverting input of the operational amplifier, sends a voltage signal (pulse) of $5V_{dc}$. The rising edge of the pulse causes a positive variation, which is amplified, causing a voltage V_o . Thus, the voltage on the resistor R_4 increases proportionally, making the power difference between the inputs of the opamp tend to zero again. In the case of the falling edge of the pulse, the reverse occurs.

5) SURFACE COUPLING

The reception of data on the surface is executed by the coupling circuit, which can be divided into two stages. The first is the filtering of signals at the fundamental frequency (50/60 Hz) to extract the DC current signal with the information of the parameters read. The DC current signal then passes through the current-voltage converter circuit, and its output provides a sign with the same amplitude and frequency as the signal emitted by the sub-surface microcontroller. The following topics detail each of these steps.

6) CURRENT TO VOLTAGE CONVERTER (I/V)

After removing the fundamental frequency, the modulated signal is converted back into a voltage output. The proposed I/V converter circuit consists of three stages (Figure 18). In the first, a closed-loop current transducer using the Hall effect technology, the LA 50-p / SP55, provides an output voltage proportional to the current flowing through the sensor. The operational amplifiers U_1 , U_2 and U_3 remove the DC offset signal from the previous step. The sign is amplified (opamp U_4) and sent to a comparator (Schmidt Trigger - CI 4093), which saturates the signals at the high and low levels. The comparator output, which is the output of the I/V converter, delivers the signals with their original properties to the receiving microcontroller.

C. RECEIVER DEVICE

The defined receiver module has one microcontroller unit (MCU) responsible for making the information from downhole parameters available in a Modbus bus network to industrial systems such as PLC (Programmable Logic Controller).

The main components of the receiver module are the PIC 18F4550 microcontroller, which implements the Tx-Rx and

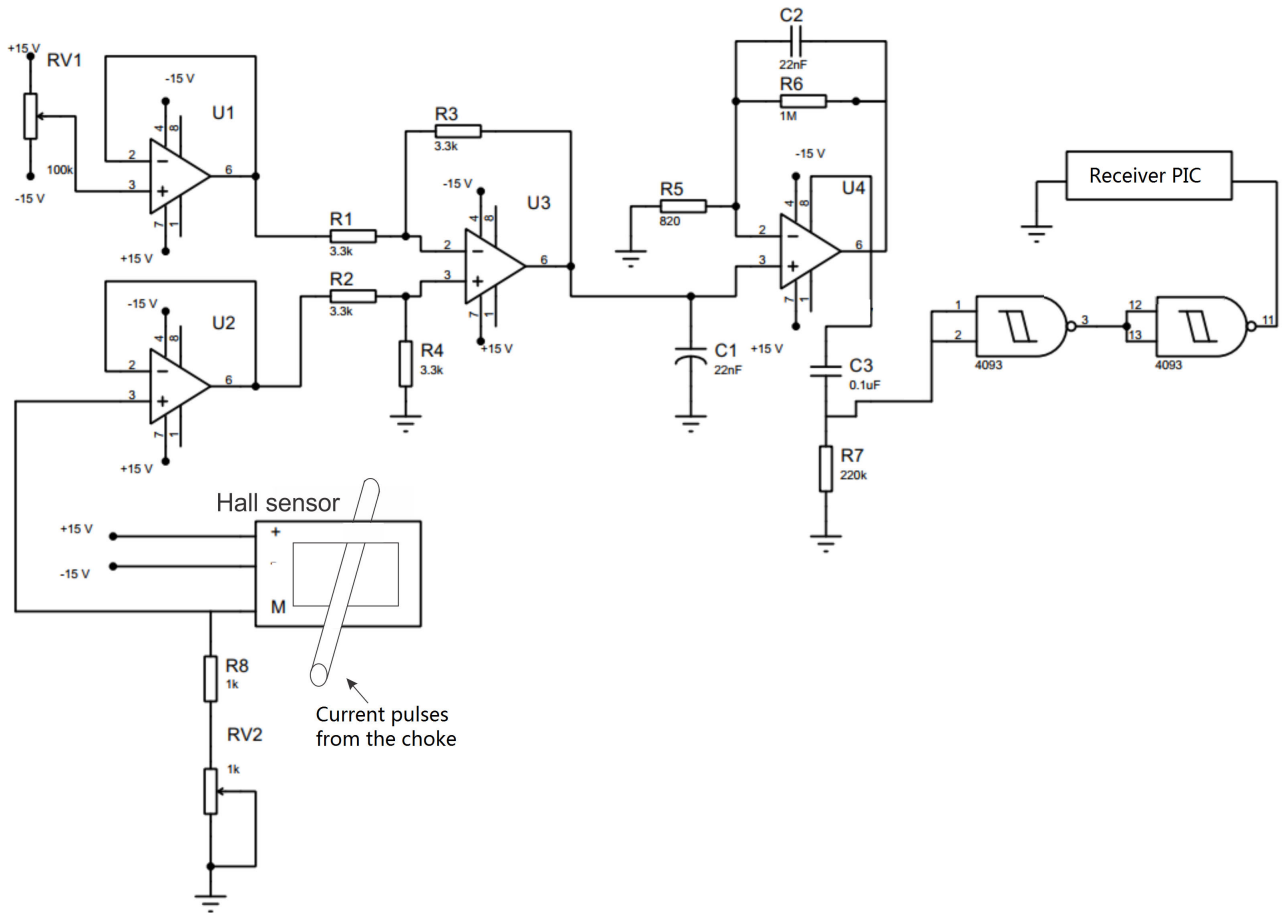


FIGURE 18. Circuit diagram for current to voltage converter.

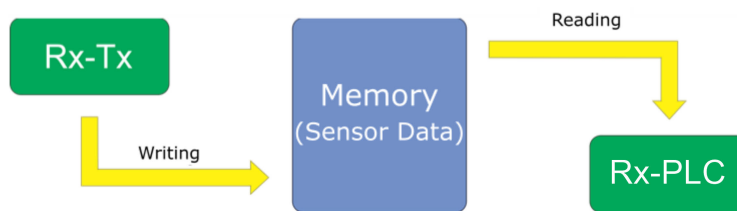


FIGURE 19. Sharing memory between the writing and reading stage.

Rx-PLC logics, an SRAM serial memory for sensor data storage, a MAX485 transceiver as an interface to the RS-485 standard, a MAX232 transceiver and various components such as capacitors, resistors, and terminals.

The receiver is configuring to attend two main tasks: the first one deals with the communication with the transmitter module, called Rx-Tx, and the second task, referred to as Rx-PLC, is responsible for the connection with the industrial devices. These two demands were implemented in order to share a single memory space, where Rx-Tx records the sensor data in that space, and the Rx-PLC part accesses them to make them available, as shown in Figure 19.

The availability of the data collected for industrial equipment is in charge of the receiver’s Rx-PLC segment, which implements the Modbus-RTU protocol with physical layer RS-485. The memory map to be accessed by industrial equipment is organized according to the Figure 20, where positions 0 to 3.999 are samples of the X-axis, 4.000 to 7.999 of the Y-axis, position 8000 indicates the number of sets of 4 thousand points (X; Y) that have already been made available and from 8.001 to 8.016 is used to store data from up to 16 regular sensors. In Figure 20, sensors of the special type represent accelerometers, while regular sensors correspond to pressure, temperature, and contamination.

The implemented Modbus protocol is configured as follows:

- Operation mode: slave;
- Slave address: 1;
- Data structure type: holding register;
- Transmission mode: serial RTU;
- Inter character timeout: 70 ms;
- Baud rate: 9600 bps;
- Parity: none;
- Stop bit: 1;
- Data bits: 8;
- RTC/CTS: none.

The slave address and baud rate can be configured through a dedicated interface. All other configuration properties can be modified, however, only modifying and compiling the source code. Because the Modbus data structure that stores the sensor data is of the holding register type, the PLC must execute read requests with function code 0×03 . Due to protocol limitations, up to 127 memory locations can be requested at a time. In this application, the Modbus protocol uses the data structure of the holding register type to store the sensor data. Therefore, the PLC must execute reading requests using the function code 0×03 . Due to protocol limitations, up to 127 memory locations can be requested at a time. Figure 20 shows the memory addresses available for reading the PLC. In this way, the requests for readings of the regular sensors by the PLC must obey the structure of the Figure 21. The previous Figure depicts an example of requesting the regular sensor stored at address 8.001.

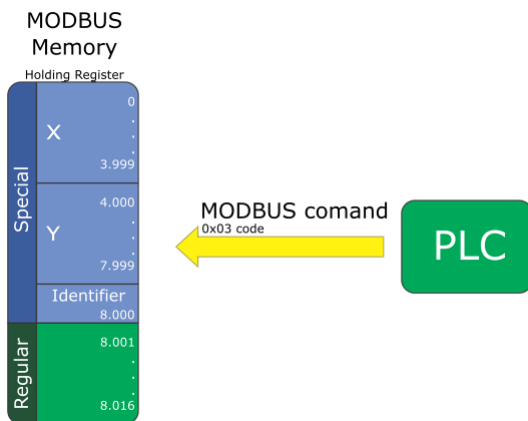


FIGURE 20. Modbus memory map.

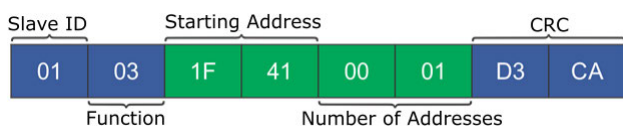


FIGURE 21. Example of modbus request for regular sensors.

Considering the special sensors, the PLC must monitor address 8.000 (identifier) to detect changes in its value.

The identifier acts as a counter for how many sets of 4 thousand points have already been made available for reading. Therefore, the increase in this field means that a new set of 4 thousand points is available to be read. Figure 22 exemplifies a request for reading the first 100 samples of the X-axis.

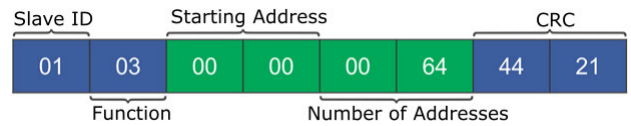


FIGURE 22. Example of modbus request for special sensors.

MEMORY ORGANIZATION

The memory described here deals only with information related to the sensors, having no relation to aspects of the source code of the device. Considering that information from special sensors requires 4 thousand samples per axis and only one is necessary for regulars, the memory was ordered according to Figure 23.

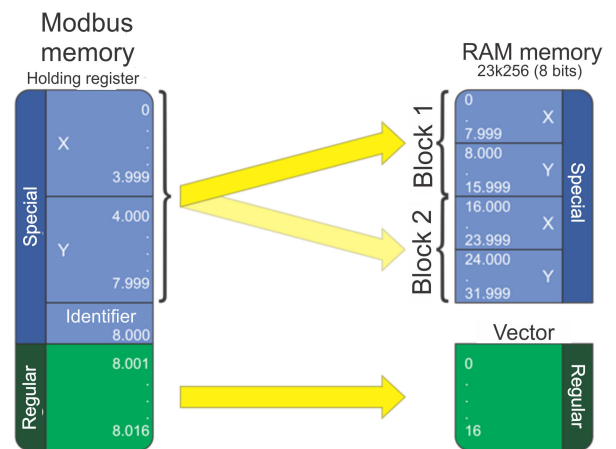


FIGURE 23. Memory organization.

The mapping of 8 thousand Modbus addresses to 16 thousand addresses in the SRAM memory results from the fact that the Modbus addresses have 16 bits and those of the SRAM memory only 8 bits. Therefore, two memory locations are required for each Modbus position. As for regular sensors, the mapping is done directly, since both structures use 16 bits. The creation of two blocks allows us to read the sensor data at the same time that the new ones are stored. This way, while the PLC is reading a set of 4,000 points in one block, the receiver module is storing a new set of 4,000 points in the other block. When filling a block, the receiver increments the identifier, which indicates which block is ready for reading and begins the process of filling in the next. Thus, the reading and writing processes continue to alternate between blocks 1 and 2.

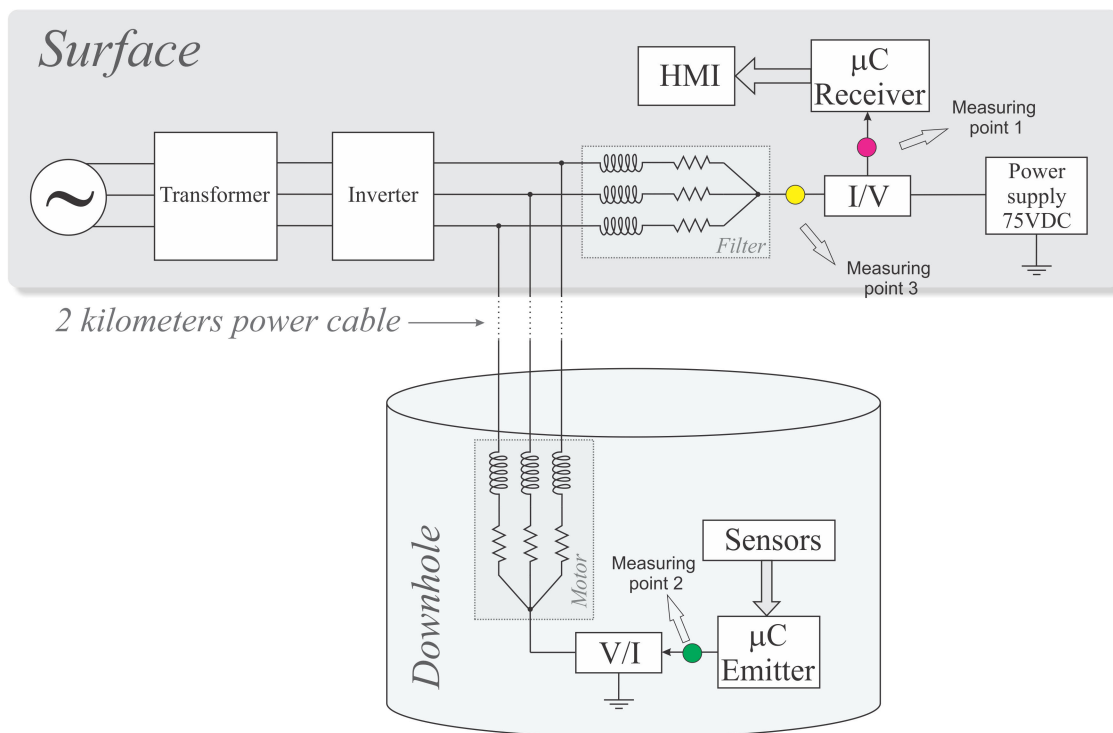


FIGURE 24. Panoramic view of the ESP structure used in the tests and the measurements points.

III. RESULTS

In this section, in order to validate the developed telemetry system, the experimental results are now exposed. The testing consisted primarily of transmitting information of three analog sensors and a digital sensor. In the experiments, the behavior of the signal during the sending of data for different motor speeds is evaluated.

A. FIELD DATA TRANSFER TEST WITH ESP SYSTEM IN OPERATION

In order to verify the behavior of the current signal sent by the emitter module along the three-phase cable and in an environment without noise, at the first moment, a test was performed with the system de-energized. Due to the simplicity of this first test and the possibility to monitor possible causes of communication failure, it was decided not to use the well structure, but to work with the ESP motor-pump assembly horizontally, connected to the 2,236-meter long cable still wound on the coil and connected to the surface filter.

The equipment used was: prototype of the transmitter module, three protection inductors connected in series, ESP pump and motor, three-phase cable with 2,236 meters, choke and receiver module. The Figure 24, which will serve as the basis for the following tests, gives a panoramic view of how the ESP equipment is arranged and the measurements points.

The points shown in Figure 24 highlight the locations for monitoring the signals. Therefore, prototypes are evaluated based on the analysis of the behavior of the signals sent and received and the voltage in the motor neutral. The result of

this test (Figure 25) showed the expected behavior, which is the reproduction on the surface of the signal sent by the bottom module, verifying that the functionality of the developed equipment was proven. It is observed that in this case, both signals have no signs of noise that could compromise the sending of information. These characteristics are due to the fact that the ESP system is not connected to the three-phase supply.

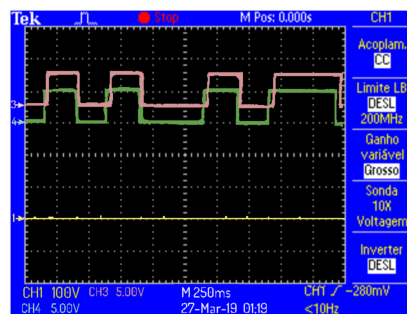


FIGURE 25. The signals of the sent and received data, and the voltage at the motor neutral for the inverter de-energized. In green is the sent signal, the pink is the received one and the yellow refer to the voltage value in the motor neutral.

Around 50 packages of regular variables (pressure, temperature and vibration) were sent, all being monitored by the Hercules SETUP tool. Figure 26 displays a terminal screen where information such as frame size, values of received variables, number of packets received with and without error, Modbus registers, among others, are presented.

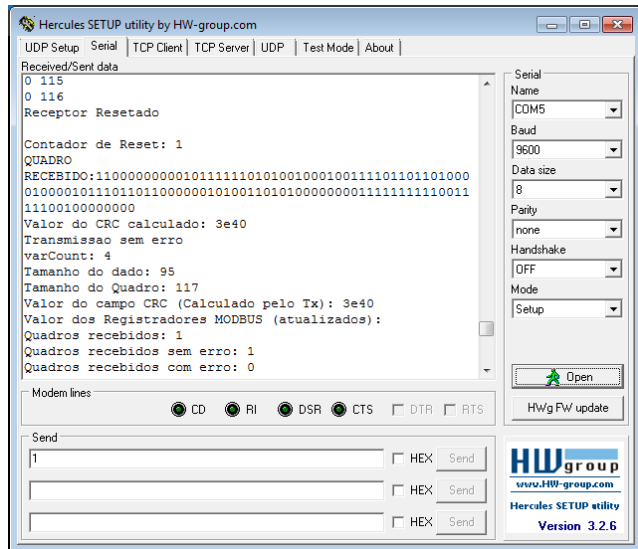


FIGURE 26. Monitoring of the received data.

The experimental arrangement of the previous step was coupled with the ESP power stages: step-down transformer, frequency inverter, and step-up transformer. The present test reproduces the previous experiment, considering the ESP system energized, however not operating. The purpose is to verify the influence of the three-phase network on the communication channel. All packets sent were received without error.

The motor is from Baker Hughes company, model FMHXG with a power of 62 HP and voltage of 1170 V. The pump also manufactured by Baker Hughes, model P4 PMXSSD 400 series with 70 stages. The cable is Prysmian, model EPDM / LEAD / GSTA, 2,236 meters long, 2 AWG ($33,6 \text{ mm}^2$), and flat configurations. The purpose of this test is to evaluate the behavior of the communication modules with the ESP system in operation and subjected to a variation of the motor's operating frequency. Therefore, the emitter and receiver were only started after the ESP motor was launched at a frequency of 10 Hz. The transition between the frequency values occurred dynamically, that is, with the system in operation, ranging from 10 to 59.8 Hz.

The Figures 27 and 28 show screenshots of the oscilloscope of the test described for 30 Hz and 60 Hz. Channel 4 of the oscilloscope, in green, represents the signal at the transmitter, the pink wave the sign at the receiver, and the yellow wave reproduces the behavior of the voltage at the motor neutral. The idea of monitoring this voltage is to protect the electronic boards and prevent accidents, as an imbalance in the motor phases would produce a relatively high voltage. It can be seen in the image that the scale of this wave is at 100V per division.

The result shows a voltage oscillations in the motor neutral. However, despite this voltage variation, the digital signals referring to the sent and received data did not present any noise effects. The test lasted 30 minutes, and the results achieved showed no transmission error for any frequency value.

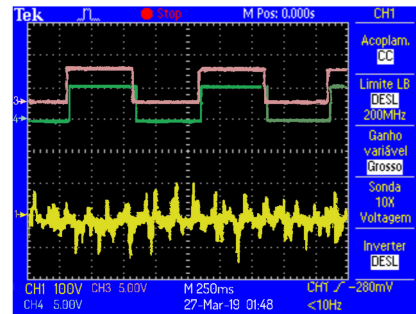


FIGURE 27. The six pulse VSD operating at 30 Hz. waveform using the baker hughes 6-pulse inverter[®]. VSD operating at 30 Hz. In green is the sent signal, the pink is the received one and the yellow refer to the voltage value in the motor neutral.

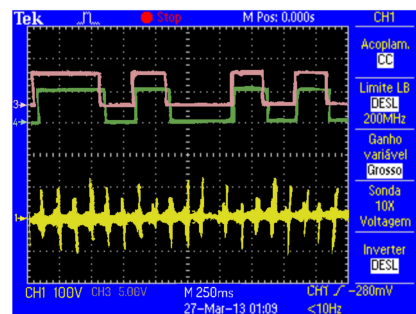


FIGURE 28. The six pulse VSD operating at 60 Hz. waveform using the baker hughes 6-pulse inverter[®]. VSD operating at 60 Hz. In green is the sent signal, the pink is the received one and the yellow refer to the voltage value in the motor neutral.

Following the same profile, the fourth test considered the same structure, except the frequency inverter. The experimental setup utilizes now a VSD manufactured by Schneider Electric[®], Altivar 61 model, PWM type, which provides the motor with a supply voltage closer to the sinusoidal. Compared to the 6-pulse converter, PWM has, among other advantages, the ability to inject less noise into the network. An active filter, Schneider Electric[®], is also integrated into the same drive panel as the Schneider Electric inverter Accusine model. Despite the existence of this tool that would reduce the disturbances caused by the inverter, it was decided in a first step to leaving it decoupled, to evaluate only the influence of the PWM converter.

This test provides, as well as the previous one, to evaluate the behavior of the signals involved in the transmission, considering an increase of the motor rotation frequency. The motor was started at a low frequency of 30 Hz and was it increased from 5 Hz to 5 Hz until reaching 60 Hz. The packet sending process started after the engine started at low frequency. The test lasted 2 hours, with 120 data packets being sent. Figures 29 and 30 illustrate parts of the signals being sent and received for the frequencies of 30 Hz and 60 Hz, respectively. The signal captured at the transmitter is green, the pink signal refers to the receiver and the yellow signal to the neutral voltage.

As seen in Figures 29 and 30, the monitored signals have virtually no interference from noise. This behavior is mainly

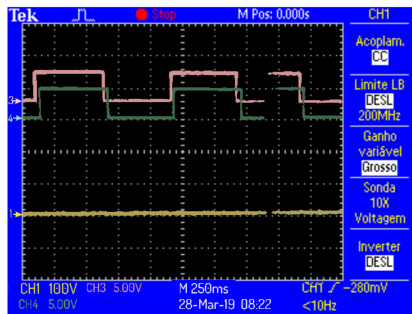


FIGURE 29. Waveform obtained using the PWM inverter *Schneider*[®]: VSD operating at 30 Hz. In green is the sent signal, the pink is the received one and the yellow refer to the voltage value in the motor neutral.

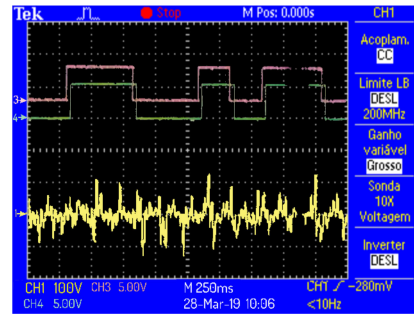


FIGURE 32. The signals of the sent and received data, and the voltage at the motor neutral at low frequencies during ESP startup with Accusine active filter. In green is the sent signal, the pink is the received one and the yellow refer to the voltage value in the motor neutral.

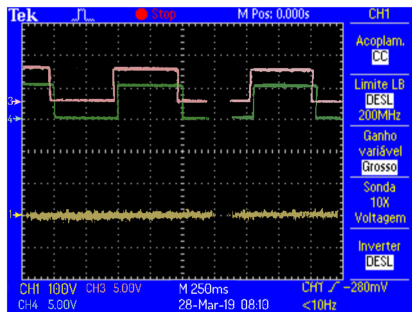


FIGURE 30. Waveform obtained using the PWM inverter *Schneider*[®]: VSD operating at 60 Hz. In green is the sent signal, the pink is the received one and the yellow refer to the voltage value in the motor neutral.

due to the PWM inverter quality, which injects less noise into the motor supply line and the cable shield. The increment of the noise of motors supplied from PWM controlled inverters compared with the same one supplied from a sinusoidal supply is relatively small. The engine shutdown caused the generation of a high amplitude impulsive noise (from -300 to 300 V) at the neutral point. The cause for noise with impulsive and short-lived characteristics is due to the instantaneous unbalance of the voltage in the motor winding. Despite the high voltage amplitude in the neutral, the printed circuit boards have not been damaged. Figure 31 highlights this event.

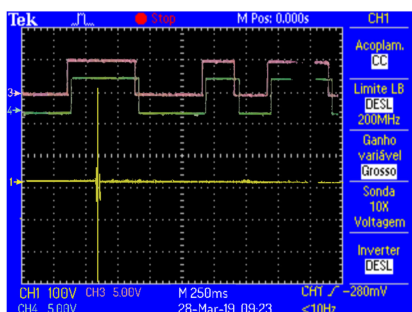


FIGURE 31. Peak voltage in neutral after switching off the PWM inverter.

Finally, the prototypes were subjected to the starting conditions of the well with ESP. The structure of the previous test

was maintained. However, added the Accusine active filter from Schneider Electric[®]. This test aims to analyze how the signals behave during the transient of the activation, in which the channel presents as a very noisy characteristic behavior. Also lasting 40 minutes, the test showed no error in any of the packets sent, including at the critical moment of activation. In Figure 32 it is possible to see the behavior of the neutral voltage in the motor and of the signals sent and received for a frequency of 6.3 Hz during the startup of the ESP system.

IV. CONCLUSION

The favorable results achieved allowed the evaluation of the prototypes' performance under the conditions found in an ESP well. The equipment installed in the ESP wells provided a favorable channel for data transfer. The inductance of the motor winding acts as a filter for high frequencies, eliminating the noise associated with it but leaving only the medium and low AC frequency. The shielded cable, built especially for the ESP protects, or as the name suggests, shields the channel against the effects of electromagnetic interference. In the absence of extra protection, cables can act both as a source, conducting noise to other equipment, as well as a receiver or antenna, capturing radiated EMI from other sources. The active filter installed for each phase at the inverter output is characterized as a low-pass filter and has a cutoff frequency between the output AC frequency and the PWM frequency of the inverter. Therefore, an active filter provides a channel free of harmonic currents caused by non-linear loads. Also, as could be observed in the test that considered the filter active, the voltage in the neutral had a low oscillation, which is due to the ability of the filter to balance the voltage values that reach the motor.

The proposed communication protocol ensure determinism and reliability during the data transfer between the sending and receiving devices. The implementation of two frames of different sizes made it possible to send regular variables (pressure, temperature, and contamination) and vibration data. Manchester encoding enabled synchronization between the bottom and surface modules, and the CRC error detection

method, typically used in digital networks, was used to verify the integrity of the packets.

One of the main contributions of this article is to present a hardware and software solution for monitoring the subsurface parameters of the ESP artificial lift method. In summary, the evaluation results for the first tests showed the reliability and robustness of the proposed telemetry system. The transfer rate of 5 to 10 bps, considered low compared to other telemetry/communication systems, is sufficient for applications such as reading sensors to adjust production and collecting information for predictive maintenance, considering the slow dynamics of ESP.

REFERENCES

- [1] S. Quintero, S. Figueiredo, V. Takahashi, R. Llerena, and A. Braga, "Passive downhole pressure sensor based on surface acoustic wave technology," *Sensors*, vol. 17, no. 7, p. 1635, Jul. 2017.
- [2] N. Song, M. Wang, B. Dang, S. Liu, and Z. Ren, "Real-time monitoring system of leakage current for electric submersible pump," *IOP Conf. Ser., Mater. Sci. Eng.*, vol. 799, May 2020, Art. no. 012008.
- [3] J. Han and Q. Gao, "Research on downhole multi-parameters monitoring system," in *Proc. 7th Int. Power Electron. Motion Control Conf.*, Jun. 2012, pp. 2765–2768.
- [4] L. Li, C. Hua, and X. Xu, "Condition monitoring and fault diagnosis of electric submersible pump based on wellhead electrical parameters and production parameters," *Syst. Sci. Control Eng.*, vol. 6, no. 3, pp. 253–261, Sep. 2018.
- [5] M. Hackworth and S. Williams, "Real-time decision making for ESP management and optimization," presented at the SPE North Amer. Artif. Lift Conf. Exhib., The Woodlands, TX, USA, Oct. 2016, doi: 10.2118/181219-MS.
- [6] S. Spagnolo, S. Pilonè, and L. Corti, "Fully retrievable ESP: A new artificial lift concept," in *Proc. Int. Petroleum Technol. Conf.*, Beijing, China: SPE, China, 2013, p. 350.
- [7] R. Bates, C. Cosad, L. Fielder, A. Kosmala, S. Hudson, G. Romero, and V. Shanmugam, "Taking the pulse of production wells—ESP surveillance," *Oilfield Rev.*, vol. 16, no. 2, pp. 16–25, 2004.
- [8] R. Flatern, *The Defining Series: Electrical Submersible Pumps*. Houston, TX, USA: Schlumberger, 2015.
- [9] X. Liang and E. Fleming, "Electrical submersible pump systems: Evaluating their power consumption," *IEEE Ind. Appl. Mag.*, vol. 19, no. 6, pp. 46–55, Nov. 2013.
- [10] X. Liang, J. He, and L. Du, "Electrical submersible pump system grounding: Current practice and future trend," *IEEE Trans. Ind. Appl.*, vol. 51, no. 6, pp. 5030–5037, Nov. 2015.
- [11] X. Liang and W. Xu, "Downhole monitoring tool design using power line disturbances," in *Proc. IEEE/IAS 51st Ind. Commercial Power Syst. Tech. Conf. (I&CPS)*, May 2015, pp. 1–11.
- [12] X. Liang, O. Ghoreishi, and W. Xu, "Downhole tool design for conditional monitoring of electrical submersible motors in oil field facilities," *IEEE Trans. Ind. Appl.*, vol. 53, no. 3, pp. 3164–3174, May 2017.
- [13] O. Ghoreishi, X. Liang, and W. Xu, "Phase-to-phase communication scheme for downhole monitoring tool design in electrical submersible pump systems," *IEEE Trans. Ind. Appl.*, vol. 52, no. 3, pp. 2077–2087, May 2016.
- [14] C. Bremner, G. Harris, A. Kosmala, B. Nicholson, A. Ollre, M. Percy, C. Salmas, and S. Solanki, "Evolving technologies: Electrical submersible pumps," *Oilfield Rev.*, vol. 18, no. 4, pp. 30–43, 2006.
- [15] T. R. Brinner, J. D. Atkins, and M. O. Durham, "Electric submersible pump grounding," *IEEE Trans. Ind. Appl.*, vol. 40, no. 5, pp. 1418–1426, Sep. 2004.
- [16] T. R. Brinner and R. A. Durham, "Transient-voltage aspects of grounding," *IEEE Trans. Ind. Appl.*, vol. 46, no. 5, pp. 1796–1804, Sep. 2010.
- [17] J. Miaoxin, G. Qiang, and X. Dianguo, "A downhole multi-parameter monitoring system," in *Proc. 3rd Int. Conf. Instrum., Meas., Comput., Commun. Control*, Sep. 2013, pp. 1660–1663.
- [18] Y. Qureshi, G. P. P. Gunaratne, and K. Christidis, "Dynamic impedance matching of transmission cables for downhole tools," in *Proc. IEE Seminar Online Monit. Techn. Off-Shore Ind.*, Aberdeen, U.K., 1999, pp. 12/1–12/5, doi: 10.1049/ic:19990731.
- [19] D. Fonsêca, A. Salazar, T. Gonçalves, and E. Villarreal, "Electrical modelling of an electrical submersible pump system three-phase power cable used in power line communication," *Przegląd Elektrotechniczny*, vol. 10, no. 3, pp. 22–26, 2019.
- [20] X. Liang, N. C. Kar, and J. Liu, "Load filter design method for medium-voltage drive applications in electrical submersible pump systems," *IEEE Trans. Ind. Appl.*, vol. 51, no. 3, pp. 2017–2029, May 2015.
- [21] N. K. Mitra, *Principles of Artificial Lift*, 1st ed. Bengaluru, India: Allied Publishers Pvt, 2012. Accessed: Nov. 20, 2020. [Online]. Available: <https://books.google.com.br/books?id=6NokTvD4mjoC>
- [22] J. Miaoxin, Z. Wei, G. Qiang, and X. Dianguo, "An ESP downhole parameters monitoring system based on current loop transmission method," in *Proc. Int. Power Electron. Conf. (IPEC-Hiroshima - ECCE ASIA)*, May 2014, pp. 3050–3054.
- [23] Y. Lv, Q. Gao, and D. Xu, "Study on downhole multi-sensor monitoring and data transmission of electric submersible pump," in *Proc. 1st Int. Conf. Instrum., Meas., Comput., Commun. Control*, Oct. 2011, pp. 70–73.
- [24] P. Zhang, Q. Gao, L. Cheng, and D. Xu, "Research on downhole multi-parameter comprehensive measurement of ESP," in *Proc. 4th Int. Conf. Instrum. Meas., Comput., Commun. Control*, Sep. 2014, pp. 346–350.
- [25] F. Quintaes, A. O. Salazar, A. L. Maitelli, F. Fontes, M. A. A. Vieira, and T. Esilley, "Magnetic sensor used to detect contamination of insulating oil in motors applied to electrical submersible pump," *IEEE Trans. Magn.*, vol. 47, no. 10, pp. 3756–3759, Oct. 2011.



DIEGO ANTONIO DE MOURA FONSECA was born in Natal, Rio Grande do Norte, Brazil. He received the degree in computer engineering from the Federal University of Rio Grande do Norte, in 2007, and the master's degree in electrical and computer engineering from the Federal University of Rio Grande do Norte, in 2011. He is currently a Computer Engineer with the Federal University of Rio Grande do Norte. His current research interests include computer engineering, with emphasis on electronic automation of industrial processes, acting mainly on the following themes: instrumentation, industrial automation, and programming.



ANDRÉS ORTIZ SALAZAR (Member, IEEE) was born in Lima, Peru. He received the degree in electronic engineering from the National University of Engineering, Lima, and the master's degree in electric engineering and the Ph.D. degree in electric engineering from the Federal University of Rio de Janeiro, Brazil, in 1989 and 1994, respectively. He held a postdoctoral position in electric engineering with the Tokyo University of Science, SUT, Japan, in 2000. He has been a Teacher with the Federal University of Rio Grande do Norte, since 1994, where teaches instrumentation, industrial automation, power electronics, machine activation, and automation. His researches are concentrated on the Electronic Automation of Electrical and Industrial Processes.



ELMER ROLANDO LLANOS VILLARREAL (Member, IEEE) was born in Huánuco, Peru. He received the B.Sc. degree in mathematics from the National University of Engineering, Lima, Peru, the master's degree in electric engineering from the Polytechnic School University of Sao Paulo, in 1997, and the Ph.D. degree in electric engineering from the Federal University of Santa Catarina, Brazil, in 2002. In 2019, he held a postdoctoral position in electric engineering with the Federal University of Rio Grande do Norte. Since 2009, he has been a Teacher with the Federal Rural University of the Semi-Arid, where teaches linear algebra, linear systems, and numerical calculus. His researches are concentrated on the Mathematical Modeling and control system.



GERMAN ALBERTO ECHAIZ ESPINOZA was born Arequipa, Peru. He received the degree in electronic engineering from the National University of Engineering, Lima, Peru, the master's degree in instrumentation and control, and the Ph.D. degree in energy engineering from the Universidad Nacional de San Agustín de Arequipa, Arequipa, Peru. He is currently the Director of the Academic Department of Electronic Engineering, Universidad Nacional de San Agustín de Arequipa.



ALAN CÁSSIO QUEIROZ BEZERRA LEITE was born in Mossoró, Rio Grande do Norte, Brazil. He received the degree in electrical engineering from the Federal University of Rio Grande do Norte. He was a Technician in electrotechnics from the Federal Institute of Rio Grande do Norte. He was also a Substitute Professor of higher teaching with the School of Sciences and Technologies, Federal University of Rio Grande do Norte, and also with the Department of Communications Engineering. Has to experience in electrical engineering, with emphasis on automation of electrical systems and photovoltaic energy.

• • •